

Dynamic Stability of an Axially Moving Sandwich Composite Web

Krzysztof MARYNOWSKI
Department of Dynamics of Machines

Zbigniew KOŁAKOWSKI
*Department of Strength of Materials and Structures
Technical University of Łódź, 90-924 Łódź, ul Stefanowskiego 1/15, Poland*

Received (19 August 2003)
Revised (22 September 2003)
Accepted (1 December 2003)

Dynamic stability of an axially moving corrugated board web has been investigated. The board web is modelled as an thin-walled composite plate structure. Mathematical model of the moving web system has been derived using the classical laminated panel theory. In the solution of the problem the Koiter's asymptotic expansion and the numerical transition matrix method have been employed: The results of numerical investigations show the solutions to the linearized problem. The effects of the transport velocity and axial load of the web on its dynamic stability are presented.

Keywords: thin wall structures, moving web, composite materials.

1. Introduction

Since their appearance in the 1960's, the use of modern composite materials is growing rapidly around the world. Composites have been lately commonly used in aircraft industry, army, automotive industry and marine structures, as well as in packaging. With progress in the technology of composite materials, composite plates made of solid laminates, sandwich laminates, and laminates reinforced with stiffeners are widely used in packages, cars, wagons, ships, aeroplanes and marine structures. The positive factors promoting the use of fibrous composites in the construction of load carrying elements include good wear (e.g. friction) resistance, fatigue life (under time-variable loads), sound insulation properties or electromagnetic transparency.

Corrugated board is a highly efficient composite material. It is used extensively as a packaging material because of its high strength and stiffness properties. These properties allow it to be manufactured into boxes and trays for transporting, storing and distributing a wide range of consumer products.

Paper and corrugated board properties derive from the raw materials and papermaking processes. Relatively recent technical developments allow high speed formation of the web in simultaneous or sequential multi-layered structure like paperboard. Paper is generally considered to be an anisotropic fibrous composite material. Theoretical models describing mechanical properties of paperboard including those based on a thin-walled orthotropic plate structure.

Excessive vibrations of moving board webs in the industry increase the defects and can lead to failure of the web. In the paper and textile industries involving motion of thin materials, stress analysis in the moving web is essential for the control of wrinkle, flutter and sheet break. Although the mechanical behaviour of axially moving materials has been studied for many years, little information is available on the dynamic behaviour and stress distribution in the axially moving multi-layered paper and board materials.

A lot of earlier works in this field focussed on investigations of stationary orthotropic composite plates. A more comprehensive review of the literature can be found in investigations of Dawe and Wang [3], Jones [4], Kolakowski and Królak [7], Loughlan [10, 11], Matsunga [12], Walker et al. [17], Wang et al. [18].

On the other hand, in literature one can find a lot of works on dynamic investigations of axially moving orthotropic web, i.e. one-layered systems. Recent works in this field analysed the non-linear vibrations of an axially moving orthotropic web [13, 14], the equilibrium displacement and stress distribution in non-linear model of an axially moving plate [9], the wrinkling phenomenon and stability of the linear model of an axially moving isotropic plate [8], and stress distribution in an axially moving plate [19].

The aim of this paper is to analyse the dynamic stability of an axially moving sandwich composite web. Mathematical model of the moving web system has been derived using the classical laminated panel theory. In the solution of the problem the Koiter's asymptotic expansion and the numerical transition matrix method have been employed: Numerical investigations are carried out for a corrugated board composite structure. The numerical data of the board material received on the base of experimental investigations have been taken from the recent literature. Paperboard is treated as thin-walled composite structure in the elastic range, being under axial extension. The effects of the transport velocity and axial load of the web on its dynamic stability are presented in this paper.

2. Formulation of the problem

Three-layered composites consist of two thin facings (the skin or sheets) sandwiching a core (Fig. 1). The facings are made of high strength materials having good properties under tension while the siding core in the form of corrugated trapezoidal plate is made of lightweight materials. Sandwich composites combine lightness and flexural stiffness. Fig. 1 also depicts the coordinate system. The x -axis refers to the machine direction, the y -axis refers to the cross or transverse direction. The machine and cross directions form the plane of the structure, and z -axis refers to the out-of-plane (or through- thickness) direction.

Let us consider thin-walled web built of plate elements (panels). The web under consideration is multi-layer plate made of orthotropic materials. The composite

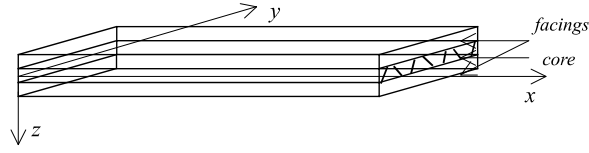


Figure 1 Schematic of the sandwich composite macrostructure

has been modeled as the thin-walled laminar construction with rigid core. The classical laminated panel theory [4] is used in the theoretical analysis, the effects of shear deformation through the thickness of the laminate are neglected and the results given are those for thin laminated panels. The materials they are made of are subjected to Hooke's law.

For each panel component, precise geometrical relationships are assumed in order to enable the consideration of both out-of-plane and in-plane bending of the plate:

$$\begin{aligned}
 \varepsilon_1 &= u_{1,1} + 0.5u_{m,1}u_{m,1} \\
 \varepsilon_2 &= u_{2,2} + 0.5u_{m,2}u_{m,2} \\
 \varepsilon_3 &= u_{1,2} + u_{2,1} + u_{m,1}u_{m,2} \\
 \varepsilon_4 &= -hu_{3,11}; \quad \varepsilon_5 = -hu_{3,22}; \quad \varepsilon_6 = -2h u_{3,12}
 \end{aligned} \tag{1}$$

where: h is the thickness of the plate, $u_1 \equiv u$, $u_2 \equiv v$, $u_3 \equiv w$ – the components of the displacement vector in the $x_1 \equiv x$, $x_2 \equiv y$, $x_3 \equiv z$ axis direction, respectively, and $\varepsilon_1 = \varepsilon_x$, $\varepsilon_2 = \varepsilon_y$, $\varepsilon_3 = 2\varepsilon_{xy} = \gamma_{xy}$, $\varepsilon_4 = h\kappa_x$, $\varepsilon_5 = h\kappa_y$, $\varepsilon_6 = h\kappa_{xy}$. The summation with respect to the factor m is from 1 to 3 ($m = 1, 2, 3$).

Using the classical plate theory [4, 6], the constitutive equation for the laminate is taken as follows:

$$\{N\} = \begin{bmatrix} [A] & [B] \\ [B] & [D] \end{bmatrix} \{\varepsilon\} = [K] \{\varepsilon\} \tag{2}$$

where:

$$A_{ij} = \frac{1}{h} \sum_{k=1}^N (\bar{Q}_{ij})_k (z_k - z_{k-1}) \tag{3}$$

$$B_{ij} = \frac{1}{2h^2} \sum_{k=1}^N (\bar{Q}_{ij})_k (z_k^2 - z_{k-1}^2) \tag{4}$$

$$D_{ij} = \frac{1}{3h^3} \sum_{k=1}^N (\bar{Q}_{ij})_k (z_k^3 - z_{k-1}^3) \tag{5}$$

$$\begin{aligned}
 K &= \begin{bmatrix} [A] & [B] \\ [B] & [D] \end{bmatrix} \\
 &= \begin{bmatrix} A_{11} & A_{12} & A_{16} & B_{11} & B_{12} & B_{16} \\ A_{21} & A_{22} & A_{26} & B_{21} & B_{22} & B_{26} \\ A_{61} & A_{62} & A_{66} & B_{61} & B_{62} & B_{66} \\ B_{11} & B_{12} & B_{16} & D_{11} & D_{12} & D_{16} \\ B_{21} & B_{22} & B_{26} & D_{21} & D_{22} & D_{26} \\ B_{61} & B_{62} & B_{66} & D_{61} & D_{62} & D_{66} \end{bmatrix}
 \end{aligned} \tag{6}$$

$$= \begin{bmatrix} K_{11} & K_{12} & K_{13} & K_{14} & K_{15} & K_{16} \\ K_{21} & K_{22} & K_{23} & K_{24} & K_{25} & K_{26} \\ K_{31} & K_{32} & K_{33} & K_{34} & K_{35} & K_{36} \\ K_{41} & K_{42} & K_{43} & K_{44} & K_{45} & K_{46} \\ K_{51} & K_{52} & K_{53} & K_{54} & K_{55} & K_{56} \\ K_{61} & K_{62} & K_{63} & K_{64} & K_{65} & K_{66} \end{bmatrix}$$

in which $A_{ij} = A_{ji}$, $B_{ij} = B_{ji}$, $D_{ij} = D_{ji}$, $K_{ij} = K_{ji}$ and \bar{Q}_{ij} is the transformed reduced stiffness matrix.

In the above equations N_1, N_2, N_3 are the dimensionless sectional forces and N_4, N_5, N_6 – the dimensionless sectional moments:

$$N_1 = \frac{N_x}{E_0 h}; N_2 = \frac{N_y}{E_0 h}; N_3 = \frac{N_{xy}}{E_0 h}; N_4 = \frac{M_x}{E_0 h^2}; N_5 = \frac{M_y}{E_0 h^2}; N_6 = \frac{M_{xy}}{E_0 h^2}, \quad (7)$$

where E_0 is the elastic modulus of reference.

The reverse relation with respect to (2) can be written as:

$$\{\varepsilon\} = [K]^{-1} \{N\} = [\bar{K}] \{N\} \quad (8)$$

In the constitutive matrix of Eq. (2), the submatrix $[A]$, detailed in Eq. (3) and related to the in-plane response of the laminate, is called extensional stiffness. The submatrix $[D]$, described by Eq. (4), is associated with the out-of-plane bending response of the laminate and is called bending stiffness, whereas the submatrix $[B]$, illustrated by Eq. (3), is a measure of an interaction (coupling) between the membrane and the bending action. Thus, it is impossible to pull on a laminate that has B_{ij} terms without bending and/or twisting the laminate at the same time. That is, an extensional force results in not only extensional deformations, but also twisting and/or bending of the laminate. Moreover, such a laminate cannot be subjected to moment without suffering simultaneously from extension of the middle surface [3, 4, 6].

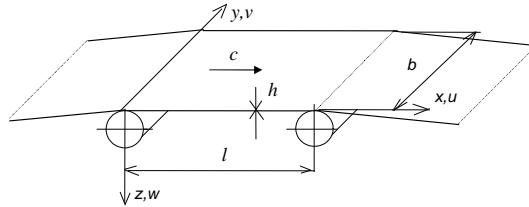


Figure 2 Axially moving web

Let suppose now that the multi-layered web of the length l is considered. The web moves at the constant velocity c in the x direction. The geometry of the considered model is shown in Fig. 2. The equations of dynamic stability of the moving composite structure have been derived using the Hamilton's principle. Actual trajectories differ from the other that satisfy the Hamilton's principle for the web can

be written as:

$$\begin{aligned} \delta \int_{t_0}^{t_1} L dt &= \int_{t_0}^{t_1} (\delta U - \delta V + \delta W) dt = \\ & \int_{t_0}^{t_1} \left\{ 0.5 \int_{\Omega} \rho \delta \left[(c + u_{1,t} + cu_{1,1})^2 + (u_{2,t} + cu_{2,1})^2 + (u_{3,t} + cu_{3,1})^2 \right] d\Omega \right. \\ & \left. - \int_{\Omega} (\sigma_1 \delta \varepsilon_1 + \sigma_2 \delta \varepsilon_2 + \sigma_3 \delta \varepsilon_3) d\Omega + \int_0^b h p^0(x_2) \delta u_1 dx_2 \Big|_{x_1=0}^{x_1=\ell} \right\} dt = 0 \end{aligned} \quad (9)$$

where: U – kinetic energy, V – internal elastic strain energy, W – work of external forces, $p^0(x_2)$ – external load in the plate middle surface. The expression $\Omega = \ell \times b \times h = S \times h$ has been employed in the above relation.

In order to determine the variation of a single multi-layer panel, the following identity has been taken

$$X \delta Y = \delta(XY) - Y \delta X. \quad (10)$$

After grouping the components at respective variations, the following system of equations of motion has been obtained:

$$\begin{aligned} & \int_{t_0}^t \int_S \left\{ [N_1(1 + u_{1,1}) + N_3 u_{1,2}]_{,1} + [N_2 u_{1,2} + N_3(1 + u_{1,1})]_{,2} + \right. \\ & \quad \left. \bar{\rho} (-u_{1,tt} - 2cu_{1,1t} - c^2 u_{1,11}) \right\} \delta u_1 dS dt = 0 \\ & \int_{t_0}^t \int_S \left\{ [N_1 u_{2,1} + N_3(1 + u_{2,2})]_{,1} + [N_2(1 + u_{2,2}) + N_3 u_{2,1}]_{,2} + \right. \\ & \quad \left. \bar{\rho} (-u_{2,tt} - 2cu_{2,1t} - c^2 u_{2,11}) \right\} \delta u_2 dS dt = 0 \\ & \int_{t_0}^t \int_S \left[(hN_{4,1} + N_1 u_{3,1} + N_3 u_{3,2})_{,1} + (hN_{5,2} + 2hN_{6,1} + N_2 u_{3,2} + N_3 u_{3,1})_{,2} + \right. \\ & \quad \left. \bar{\rho} (-u_{3,tt} - 2cu_{3,1t} - c^2 u_{3,11}) \right] \delta u_3 dS dt = 0 \end{aligned} \quad (11)$$

where:

$$\bar{\rho} = \frac{1}{h} \sum_{k=1}^N \rho_k (z_k - z_{k-1}); \quad \int_{t_0}^t \int_S [\varepsilon_i - \bar{K}_{ij} N_j] \delta N_i dS dt = 0, \quad i, j = 1, 2, \dots, 6. \quad (12)$$

The boundary conditions for $x_1=\text{const}$:

$$\begin{aligned}
& \int_{t_0}^{t_1} \int_0^b \left\{ \bar{\rho} (c^2 + c u_{1,t} + c^2 u_{1,1}) - [N_1 + N_1 u_{1,1} + N_3 u_{1,2} - h p^0(x_2)] \right\} \delta u_1 dx_2 dt \Big|_{x_1} = 0 \\
& \int_{t_0}^{t_1} \int_0^b \left\{ \bar{\rho} (c u_{2,t} + c^2 u_{2,1}) - [N_3 + N_1 u_{2,1} + N_3 u_{2,2}] \right\} \delta u_2 dx_2 dt \Big|_{x_1} = 0 \\
& \int_{t_0}^{t_1} \int_0^b N_4 \delta u_{3,1} dx_2 dt \Big|_{x_1} = 0 \\
& \int_{t_0}^{t_1} \int_0^b \left\{ \bar{\rho} (c u_{3,t} + c^2 u_{3,1}) - (h N_{4,1} + 2h N_{6,2} + N_1 u_{3,1} + N_3 u_{3,2}) \right\} \delta u_3 dx_2 dt \Big|_{x_1} = 0
\end{aligned} \tag{13}$$

The boundary conditions for $x_2=\text{const}$:

$$\begin{aligned}
& \int_{t_0}^{t_1} \int_0^l [N_2 + N_2 u_{2,2} + N_3 u_{2,1}] \delta u_2 dx_1 dt \Big|_{x_2} = 0 \\
& \int_{t_0}^{t_1} \int_0^l [N_3 + N_2 u_{1,2} + N_3 u_{1,1}] \delta u_1 dx_1 dt \Big|_{x_2} = 0 \\
& \int_{t_0}^{t_1} \int_0^l N_5 \delta u_{3,2} dx_1 dt \Big|_{x_2} = 0 \\
& \int_{t_0}^{t_1} \int_0^l (h N_{5,2} + 2h N_{6,1} + N_2 u_{3,2} + N_3 u_{3,1}) \delta u_3 dx_1 dt \Big|_{x_2} = 0
\end{aligned} \tag{14}$$

The boundary conditions for the plate corner ($x_1 = \text{const}$ and $x_2 = \text{const}$):

$$\int_{t_0}^{t_1} 2N_6 \Big|_{x_1} \Big|_{x_2} \delta u_3 dt = 0 \tag{15}$$

Initial conditions ($t = \text{const}$):

$$\begin{aligned}
& \int_0^l \int_0^b [\bar{\rho} (c + u_{1,t} + c u_{1,1})] \delta u_1 dx_1 dx_2 \Big|_t = 0 \\
& \int_0^l \int_0^b [\bar{\rho} (u_{2,t} + c u_{2,1})] \delta u_2 dx_1 dx_2 \Big|_t = 0 \\
& \int_0^l \int_0^b [\bar{\rho} (u_{3,t} + c u_{3,1})] \delta u_3 dx_1 dx_2 \Big|_t = 0
\end{aligned} \tag{16}$$

Eq. (9) is a system of equilibrium equations. Eq. (12) are the already employed relations between strains and external forces, whereas relations (10), (11) and (12) correspond to the boundary conditions and in the plate corner.

3. Solution of the problem

The problem of dynamic stability has been solved with asymptotic perturbation method. In the solution of the problem and in the computer program developed, the following have been employed: Koiter's or Byskov-Hutchinson's asymptotic

expansion [2, 5], the numerical transition matrix method using Godunov's orthogonalization method [6, 7].

As has been mentioned above, the fields of displacements \bar{U} and the fields of sectional forces \bar{N} have been expanded into power series with respect to the dimensionless amplitude of the web deflection ζ_n (the amplitude of the n -th free vibration frequency of the extension system divided by the thickness h_1 of the web assumed to be the first one):

$$\begin{aligned}\bar{U} &= \lambda \bar{U}_k^{(0)} + \zeta_n \bar{U}_k^{(n)} + \dots \\ \bar{N} &= \lambda \bar{N}_k^{(0)} + \zeta_n \bar{N}_k^{(n)} + \dots\end{aligned}\quad (17)$$

where $\bar{U}_k^{(0)}$, $\bar{N}_k^{(0)}$ are the pre-critical static fields, and $\bar{U}_k^{(n)}$, $\bar{N}_k^{(n)}$ – the first order fields for the composite k -th web.

After substitution of expansions (13) into equilibrium equations (9), continuity conditions and boundary conditions (10) ÷ (12), the boundary value problems of the zero and first order can be obtained. The zero approximation describes the pre-critical static state, whereas the first order approximation, being the linear problem of dynamic stability, allows for determination of the eigenvalues, the eigenvector and the critical speeds of the system.

In the pre-critical static state the panels are divided along their widths into several strips under uniformly distributed tensile stresses. Instead of the finite strip method, the exact transition matrix method is used in this case [6].

The inertial forces from the in-plane displacements u and v are neglected. The pre-critical solution of the k -th composite web consisting of homogeneous fields is assumed as:

$$u_{1k}^{(0)} = (x_{1k} - \ell/2)\Delta_k; \quad u_{2k}^{(0)} = -x_{2k}\Delta_k K_{12k}/K_{22k}; \quad u_{3k}^{(0)} = 0, \quad (18)$$

where Δ_k is the actual loading. This loading is specified as the product of a unit loading system and a scalar load factor Δ_k .

Inner sectional forces of the pre-critical static state for the assumed homogeneous field of displacements (14) are expressed by the following relationships:

$$\begin{aligned}\bar{N}_{1k}^{(0)} &= -(K_{11k} - K_{12k}^2/K_{22k})\Delta_k, \\ \bar{N}_{2k}^{(0)} &= 0, \\ \bar{N}_{3k}^{(0)} &= -(K_{31k} - K_{32k}K_{21k}/K_{22k})\Delta_k, \\ \bar{N}_{4k}^{(0)} &= -(K_{41k} - K_{42k}K_{21k}/K_{22k})\Delta_k, \\ \bar{N}_{5k}^{(0)} &= -(K_{51k} - K_{52k}K_{21k}/K_{22k})\Delta_k, \\ \bar{N}_{6k}^{(0)} &= -(K_{61k} - K_{62k}K_{21k}/K_{22k})\Delta_k.\end{aligned}\quad (19)$$

In the second dynamical component of the last Eqs (9) there is derivative with respect to x_1 and t . Because of the trigonometric functions incompatibility in the $x_1 \equiv x$ -direction, the Galerkin-Bubnov orthogonalization procedure has been used to find approximating solution of this equation.

Numerical aspects of the problem being solved for the first order fields have resulted in an introduction of the following new orthogonal functions with n -th harmonic for k -th composite web in the sense of the boundary conditions for two

longitudinal edges [6]:

$$\begin{aligned}
\bar{a}_k^{(n)} &= N_{2k}^{(n)}(1 + \lambda\Delta_k K_{21k}/K_{22k}) + \lambda N_{3k}^{(o)} \bar{d}_{k,\xi}^{(n)}/b_k, \\
\bar{b}_k^{(n)} &= N_{3k}^{(n)}(1 - \lambda\Delta_k) + \lambda N_{3k}^{(o)} \bar{c}_{k,\xi}^{(n)}/b_k, \\
\bar{c}_k^{(n)} &= u_{1k}^{(n)}, \\
\bar{d}_k^{(n)} &= u_{21k}^{(n)}, \\
\bar{e}_k^{(n)} &= u_{3k}^{(n)}, \\
\bar{f}_k^{(n)} &= u_{3k,\eta}^{(n)}/b_k = \bar{e}_{k,\eta}^{(n)}/b_k, \\
\bar{g}_k^{(n)} &= N_{5k}^{(n)}, \\
\bar{h}_k^{(n)} &= h_k \bar{g}_{k,\eta}^{(n)}/b_k + 2h_k N_{6k,\xi}^{(n)}/b_k + \lambda N_{3k}^{(o)} \bar{e}_{k,\xi}^{(n)}/b_k,
\end{aligned} \tag{20}$$

where $\xi_k = x_{1k}/b_k$ and $\eta_k = x_{2k}/b_k$.

The solutions of Eq. (9) corresponding to the free support at the segment ends can be written in the following form:

$$\begin{aligned}
\bar{a}_k^{(n)} &= \sum_{n=1}^N T_n(t) \bar{A}_k^{(n)}(\eta_k) \sin \frac{n\pi b_k \xi}{\ell}, \\
\bar{b}_k^{(n)} &= \sum_{n=1}^N T_n(t) \bar{B}_k^{(n)}(\eta_k) \cos \frac{n\pi b_k \xi}{\ell}, \\
\bar{c}_k^{(n)} &= \sum_{n=1}^N T_n(t) \bar{C}_k^{(n)}(\eta_k) \cos \frac{n\pi b_k \xi}{\ell}, \\
\bar{d}_k^{(n)} &= \sum_{n=1}^N T_n(t) \bar{D}_k^{(n)}(\eta_k) \sin \frac{n\pi b_k \xi}{\ell}, \\
\bar{e}_k^{(n)} &= \sum_{n=1}^N T_n(t) \bar{E}_k^{(n)}(\eta_k) \sin \frac{n\pi b_k \xi}{\ell}, \\
\bar{f}_k^{(n)} &= \sum_{n=1}^N T_n(t) \bar{F}_k^{(n)}(\eta_k) \sin \frac{n\pi b_k \xi}{\ell}, \\
\bar{g}_k^{(n)} &= \sum_{n=1}^N T_n(t) \bar{G}_k^{(n)}(\eta_k) \sin \frac{n\pi b_k \xi}{\ell}, \\
\bar{h}_k^{(n)} &= \sum_{n=1}^N T_n(t) \bar{H}_k^{(n)}(\eta_k) \sin \frac{n\pi b_k \xi}{\ell}.
\end{aligned} \tag{21}$$

$T_n(t)$ is unknown function of time and the eigenfunctions have been determined for the unmoved web (for $c=0$).

The eigenfunctions $\bar{A}_k^{(n)}$, $\bar{B}_k^{(n)}$, $\bar{C}_k^{(n)}$, $\bar{D}_k^{(n)}$, $\bar{E}_k^{(n)}$, $\bar{F}_k^{(n)}$, $\bar{G}_k^{(n)}$, $\bar{H}_k^{(n)}$ (with the n -th harmonic) are initially unknown functions that will be determined by the numerical method of transition matrices. The solution assumed in this way allows one to determine dimensionless sectional forces for the first order approximation in the

form:

$$\begin{aligned}
N_{1k}^{(n)} &= \sum_{n=1}^N T_n(t) \bar{N}_{1k}^{(n)}(\eta_k) \sin \frac{n\pi b_k \xi}{\ell}, \\
N_{2k}^{(n)} &= \sum_{n=1}^N T_n(t) \bar{N}_{21k}^{(n)}(\eta_k) \sin \frac{n\pi b_k \xi}{\ell}, \\
N_{3k}^{(n)} &= \sum_{n=1}^N T_n(t) \bar{N}_{3k}^{(n)}(\eta_k) \cos \frac{n\pi b_k \xi}{\ell}, \\
N_{4k}^{(n)} &= \sum_{n=1}^N T_n(t) \bar{N}_{41k}^{(n)}(\eta_k) \sin \frac{n\pi b_k \xi}{\ell}, \\
N_{5k}^{(n)} &= \sum_{n=1}^N T_n(t) \bar{N}_{5k}^{(n)}(\eta_k) \sin \frac{n\pi b_k \xi}{\ell}, \\
N_{6k}^{(n)} &= \sum_{n=1}^N T_n(t) \bar{N}_{6k}^{(n)}(\eta_k) \cos \frac{n\pi b_k \xi}{\ell}
\end{aligned} \tag{22}$$

The obtained system of homogeneous ordinary differential equations has been solved by the transition matrix method, having integrated numerically the equilibrium equations along the circumferential direction in order to obtain the relationships between the state vectors on two longitudinal edges. During the integration of the equations, Godunov's orthogonalization method has been employed [7]. The presented way of solution allows for carrying out a modal dynamic analysis of complex composite webs.

In system of Eqs. (9), (12) and (14) for the unmoved web, there are two components of the zero loading $\bar{N}_{1k}^{(0)}$ and $\bar{N}_{3k}^{(0)}$. The component $\bar{N}_{3k}^{(0)}$ has an insignificant effect in comparison with $\bar{N}_{1k}^{(0)}$.

The developed computer program allows for a division of each web into several or even more than 50 strips made of different materials and with various thickness. The presented solution method enables a multi-modal dynamic analysis.

Let's return to the case of moving of composite web (for $c \neq 0$). Because of the trigonometric functions incompatibility in the x_1 direction, after substituting (21) into the last Eq. (11) the Galerkin-Bubnov orthogonalization method has been used. In this way the set of N ordinary differential equations with respect to the function $T_n(t)$ can be determined in the following form:

$$\frac{d^2 T_m}{dt^2} a_{2m} + \sum_{n=1}^N \frac{dT_n}{dt} a_{1nm} + T_m a_{0m} = 0, \quad m = 1, 2, \dots, N. \tag{23}$$

Substituting the state variables into Eq. (23) one can receive the autonomous set of $2N$ first order differential equations with respect to time. On the basis of Eq. (23) one can determine eigenvalues, eigenvectors and critical speeds of the moving system.

4. Numerical results and discussion

The numerical investigations has been carried out for the moving microcorrugated board with trapezoidal flute profile. The composite has been modeled as the thin-walled laminar construction with rigid core. Under this assumption the classical laminated plate theory has been satisfied.

The middle layer of the microcorrugated board one can consider as unidirectional corrugated trapezoidal plate which is parallel to the x_1 - direction. The take-up factor of this profile is small in comparison with overall dimensions of the plate, so in the macro-mechanical analysis one can treat this layer as orthotropic plate with major principal material directions parallel to its edges [1, 6, 10]. When one analyses the corrugated plate with large number of trapezoidal segments, one can take into account an individual segment, assuming the symmetry conditions on the longitudinal edges (Fig. 3). In this case, the boundary conditions on the longitudinal edges are neglected i.e. an infinitely wide trapezoidal plate is taken into account [16].

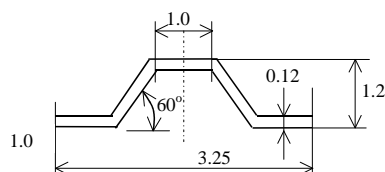


Figure 3 Cross-section of the corrugated trapezoidal plate segment

Fig. 3 shows geometric dimensions of the corrugated trapezoidal plate segment [16]. Material properties of this plate are as following: $\rho = 750[kg/m^3]$, $E_1 = E_2 = 2 \times 10^9$ [Pa], $\nu_{12} = \nu_{21} = 0.2$, $G = 0.833 \times 10^9$ [Pa]. The masses of the corrugated trapezoidal plate and the substitute orthotropic plate are the same. On the base of the condition that the stiffness of the corrugated plate and the substitute orthotropic plate are the same one receives substitute material constants,

To check above results natural frequencies of simply supported substitute orthotropic plate model have been compared with analogous values of corrugated trapezoidal plate for two different lengths $l = 1000$ mm, $l = 100$ mm for the m values: $m = 1 \div 10$. The comparison results are shown in Fig. 4.

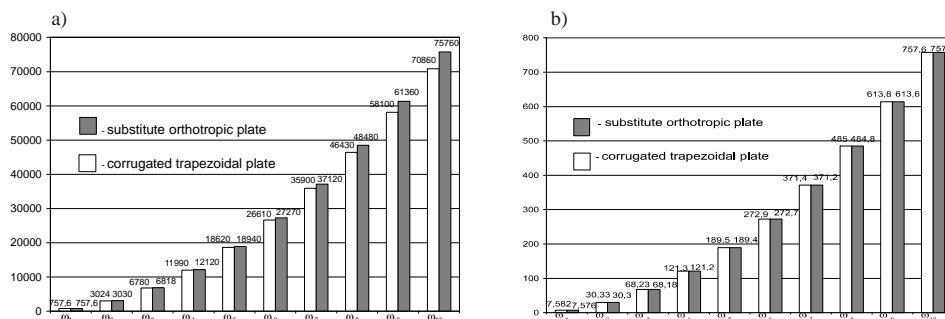


Figure 4 Natural frequencies comparison a) $l = 0.1$ m; b) $l = 1$ m

Fig. 4 shows the values of ten lowest eigenfrequencies of both compared systems for $c = 0$. These eigenvalues of both systems there are near by, but their the greatest discrepancy ($\approx 7\%$) one can observe for $l = 100$ mm and $m = 10$. Numerical data of the facing layers and the identification results as the data of the core (Fig. 1) are

Table 1 Numerical data

Length of the web l	1 m
Width of the web b	0.5 m
Thickness of the facing layer (h_F)	1.2×10^{-4} m
Thickness of the core layer h_C	1.2×10^{-3} m
Young's modulus along the machine direction and along the cross direction of the facing layer $E_{1F} = E_{2F}$	2.0 GPa
Poisson's ratio of the facing layer $\nu_{12F} = \nu_{21F}$	0.2
Shear modulus of the facing layer G_F	833.3 MPa
Mass density of the facing layer ρ_F	750.0 kg/m ³
Initial stresses N_0	5 and 10 N/m
Substitute orthotropic plate	
Young's modulus along the x axis of the core layer E_{1C}	540.0 MPa
Young's modulus along the y axis of the core layer E_{2C}	1.36 MPa
Poisson's ratio in the machine direction of the core layer ν_{12C}	0.2
Poisson's ratio in the cross direction of the core layer ν_{21C}	0.0005
Shear modulus of the core layer G_C	0.76 MPa
Mass density of the core layer ρ_C	110.0 kg/m ³

shown in Table 1.

The effect of the corrugated board properties and axial transport velocity on transverse and torsional vibrations have been studied in numerical investigations. Let σ and ω denote the real part and the imaginary part of the eigenvalues, respectively. Simultaneously ω is natural frequency of the web. The positive value of σ indicates instability of the considered system.

Dynamic investigations of axially moving systems were begun from the vibration modes definition. Fig. 5 shows the modes of two lowest flexural (ω_{11} and ω_{21}) and two lowest flexural-torsional (ω_{12} and ω_{22}) eigenfrequencies of the moving web system.

Results of dynamic stability investigations of the corrugated board system are shown in Fig. 6 and 7 for the axial load of the web $N_0 = 5$ N/m and in Fig. 8 for $N_0 = 10$ N/m. Fig. 6 shows the plot of the four lowest flexural and flexural-torsional eigenfrequencies versus the transport velocity in the pre-critical and supercritical regions of the transport speeds. The values of the imaginary part (solid line) and the real part (dotted line) of the four lowest flexural and flexural-torsional natural frequencies versus the transport velocity only in supercritical region of the transport speeds are shown in Fig. 7. The plots in Fig. 6 and 7 show that the lowest natural frequencies decrease during the axial velocity increase. At the critical transport speed the fundamental eigenfrequency vanishes indicating divergence instability (the fundamental mode with non-zero σ and zero ω).

In supercritical transport speeds ($c > c_{cr1}$), at first the web experiences a divergent instability and above that there is the second stability area where $\sigma = 0$. The width and position of the second stable region are dependent on the thickness of the composite layers. The second stable area appearance is strictly connected with the flexural and flexural-torsional eigenfrequencies distribution. In the web

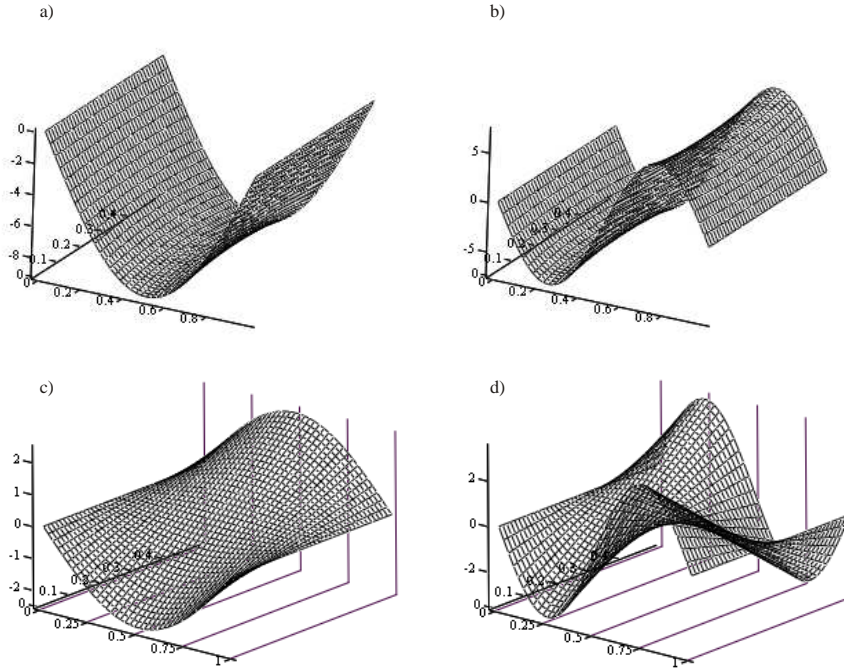


Figure 5 Non-trivial equilibrium positions of axially moving web: a) ω_{11} , b) ω_{21} , c) ω_{12} , d) ω_{22}

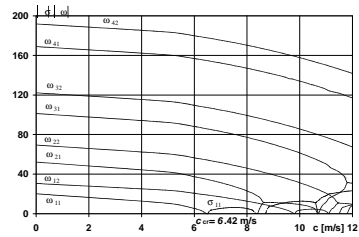


Figure 6 Flexural and flexural-torsional natural frequencies, $N_0 = 5 \text{ N/m}$

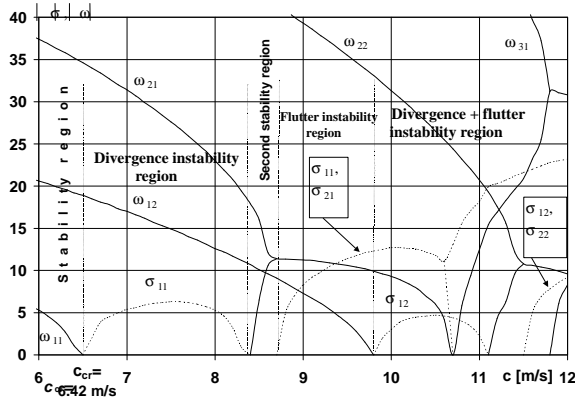


Figure 7 Flexural and flexural-torsional eigenfrequencies in supercritical region of the transport speed, $N_{x0} = 5 \text{ N/m}$

systems, where these eigenfrequencies lie near by, the second stable area does not appear at all.

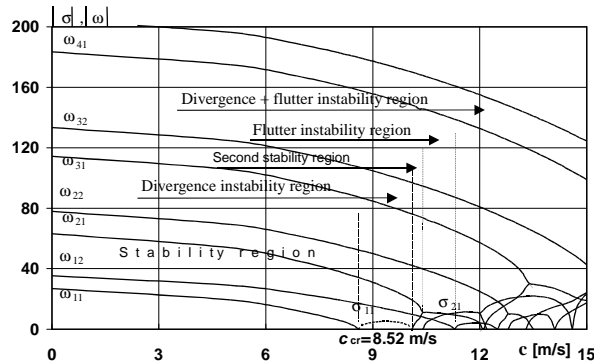


Figure 8 Flexural and flexural-torsional natural frequencies, $N_{x0} = 10 \text{ N/m}$

When the axial load of the board web increases the critical transport speed of the system increases as well. Above the second stable region at first flutter instability occurs and next flutter and divergence instability of the web motion appear.

5. Conclusions

In the paper, a new approach to the analysis of the dynamic behaviour of an axially moving sandwich composite web is presented. Mathematical model of the moving web system is derived on the basis of asymptotic perturbation method. The mathematical model solution is based on the numerical method of the transition matrix using Godunov's orthogonalization.

The numerical investigations has been carried out for the moving microcorrugated board with trapezoidal flute profile. The composite has been modeled as the thin-walled laminar construction with rigid core. Under this assumption the

classical laminated plate theory has been satisfied. The axially moving board web is treated as thin-walled composite structure in the elastic range, being under axial extension.

Calculations results of all investigated systems show in the subcritical region of transport speed for the constant axial tension of the web, the lowest flexural and flexural-torsional natural frequencies decrease during the axial velocity increase. At the critical transport speed the fundamental flexural eigenfrequency vanishes indicating divergence instability. When the axial load of the board web increases the critical transport speed of the system increases as well.

In the supercritical region of transport speed the second stable area may appear. The width and position of the second stable region are dependent on the thickness of the board layers. In the case of the paperboard webs in which the flexural and flexural-torsional eigenfrequencies lie near by, the second stable area does not appear at all.

References

- [1] **Brzoska, Z:** *Statics and stability of beam and thin-walled structures*, (1965), PWN, Warszawa, 562.
- [2] **Byskov, E and Hutchinson JW:** Mode interaction in axially stiffened cylindrical shells, *AIAA J.*, (1977), **15**, 7, 941-948.
- [3] **Dawe, DJ, Wang, S:** Buckling of composite plates and plate structures using the spline finite strip method, *Composites Engineering*, (1994), **4**, 11, 1099-1117.
- [4] **Jones, RM:** *Mechanics of composite materials*, (1975), International Student Edition, McGraw-Hill Kogakusha, Ltd., Tokyo, 365.
- [5] **Koiter, WT:** General theory of mode interaction in stiffened plate and shell structures, *WTHD, Report 590* (1976), Delft.
- [6] **Kołakowski, Z, Kowal-Michalska, K:** *Selected problems of instabilities in composite structures*, (1999), Technical University of Łódź, A series of monographs, 222.
- [7] **Kołakowski, Z, Królak, M** Interactive elastic buckling of thin-walled closed orthotropic beam-columns, *Engineering Transactions*, (1995), **43**, 4, 571-590.
- [8] **Lin, CC, Mote, CD Jr:** The wrinkling of thin, flat, rectangular webs, *Journal of Applied Mechanics ASME*, (1996), **63**, 774-779.
- [9] **Lin, CC:** Stability and vibration characteristics of axially moving plates. *Int. Journal of Solid Structures*, (1997), **34**, (24), 3179-3190.
- [10] **Loughlan, J:** The effect of membrane-flexural coupling on the compressive stability of antisymmetric angle-ply laminated plate, *Proceedings of the Third International Conference on Thin-Walled Structures*, Elsevier, (2001a), 507-514.
- [11] **Loughlan, J:** The shear buckling behaviour of thin composites plates with particular reference to the effects of bend-twist coupling, *Int. J. Mechanical Sciences*, (2001), **43**, 771-792.
- [12] **Matsunaga, H:** Buckling analysis of multilayered angle-ply composite plates, *Proceedings of the Third International Conference on Thin-Walled Structures*, (2001), Elsevier, 507-514.
- [13] **Marynowski, K, Kołakowski, Z:** Dynamic behaviour of an axially moving thin orthotropic plate, *Journal of Theoretical and Applied Mechanics*, (1999), **37**, (1), 109-128.
- [14] **Marynowski, K:** Non-linear vibrations of axially moving orthotropic web, *International Journal of Mechanics and Mechanical Engineering*, (1999), **3**, (2), 109-128.

- [15] **Savolainen, A**, (Ed.): *Paper and Paperboard Converting. Papermaking Science and Technology*, Book 12, Tappi.
- [16] **Teter, A, Kołakowski, Z**: Stability and load carrying capacity of a thin-walled corrugated trapezoidal plate, *Int. J. of Applied Mechanics and Engineering*, (2001), **6**, 2, 311-323.
- [17] **Walker, M, Adali, S, Verijenko, VE**: Optimal design of symmetric angle-ply laminates subject to nonuniform buckling loads and in-plane restraints, *Thin-Walled Structures*, (1996), **26**, 1, 45-60.
- [18] **Wang, C, Pian, THH, Dugundji, J. and Lagace, PA**: Analytical and experimental studies on the buckling of laminated thin-walled structures, *Proc. AIAA/ASME /ASCE/AHS 28th Structures, Struct. Dyn. and Materials Conf.*, (1987), Part 1, 135-140.
- [19] **Wang, X**: Numerical Analysis of Moving Orthotropic Thin Plates, *Computers & Structures*, (1999), **70**, 467-486.

